Jurnal Penelitian Fisika dan Aplikasinya (JPFA)
Volume 15, Issue 1, 12-26 2025
https://journal.unesa.ac.id/index.php/jpfa/
p-ISSN: 2087-9946
e-ISSN: 2477-1775

Utilization of Zn Powder as a Precursor in the Synthesis of rGO/ZnO Composite for Decolorization of Batik Wastewater

Dwiria Wahyuni [a,*], Mariani [b], Asifa Asri [c], Ya' Muhammad Arsyad [d]

[1] Department of Physics, Faculty of Mathematics and Natural Science, Universitas Tanjungpura, Jalan Prof. Hadari Nawawi, Pontianak 78124, Indonesia
e-mail: [a,*]dwiriawahyuni@physics.untan.ac.id, [b]anongmariani7@gmail.com, [c]asifa.asri@physics.untan.ac.id and [d]yamarsyad@gmail.com
* Corresponding Author

Received: 1 December 2024; Revised: 10 March 2025; Accepted: 28 April 2025

Abstract

Batik wastewater contains high concentrations of synthetic dyes, significantly contributing to aquatic pollution. Photocatalysis is a promising method for degrading such dyes in textile effluents. This study aims to develop rGO/ZnO composites using zinc (Zn) powder as a precursor for photocatalytic applications. Reduced graphene oxide (rGO) was used as a substrate for ZnO particle formation. The composites were prepared by reacting Zn powder with rGO at varying loadings (5% and 10% by mass) in a neutral aqueous solution, followed by thermal treatment at 250 °C for 1 hour to facilitate Zn oxidation. The photocatalytic performance was evaluated by applying different masses of rGO/ZnO (0.2, 0.4, and 0.8 g) to degrade batik wastewater. Surface morphology and elemental composition were characterized using SEM-EDS. SEM analysis showed that rGO has a sheet-like structure, while ZnO exhibits spherical morphology. EDS confirmed the presence of Zn, C, and O as major elements with Nb impurity was identified in the composite. The carbon-to-oxygen (C/O) ratio increased after composite formation, reaching 4.23 for rGO/ZnO 5% and 3.79 for rGO/ZnO 10%. XRD characterization of rGO/ZnO confirms the presence of ZnO in the composite, with residual Zn peaks indicating incomplete oxidation of the Zn precursor. Photocatalytic activities modeled using pseudo-first-order kinetics reveal the 10% rGO/ZnO composite (0.8 g) shows the degradation efficiency of 67.91%, with a rate constant of 0.1623 h^{-1}. The efficiency may be affected by the complex nature of batik wastewater, particularly wax and resin residues that hinder photocatalytic activity. In conclusion, these findings highlight the potential of Zn powder as a precursor in the synthesis of rGO/ZnO composites with concentration of rGO and the mass variation of rGO/ZnO in the treatment of Batik wastewater affect the photocatalytic activity.

Keywords: *ZnO ; rGO ; Photocatalyst ; Batik wastewater*

How to cite: Wahyuni D, Mariani, Asri A, and Arsyad YM. Utilization of Zn Powder as a Precursor in the Synthesis of rGO/ZnO Composite for Decolorization of Batik Wastewater. *Jurnal Penelitian Fisika dan Aplikasinya (JPFA)*. 2025; 15(1): 12-26. DOI: https://doi.org/10.26740/jpfa.v15n1.p12-26.

INTRODUCTION

Batik, one of Indonesia's cultural heritages, produces dyes at the coloring stage of its production [1]. Dyes in batik wastewater can degrade the quality of the aquatic environment, physically characterized by changes in turbidity, odor, color, and taste, making it unfit for daily use or sanitation [2]. The decline in water quality due to liquid batik waste causes a scarcity of clean

water, so it is not in line with the world's Sustainable Development Goal (SDGs) number 6, namely, access to clean water and sanitation. Therefore, to support the SDGs, it is necessary to treat batik wastewater before it is discharged into the aquatic environment.

A promising alternative for dye wastewater treatment is a photocatalytic process [3]–[5], in which positive holes (h+) in the valence band will be reduced by electrons in the conduction band of semiconductor materials [6]. Several semiconductor materials, such as TiO_2 [7] and ZnO [8], are commonly used as photodegradation agents to reduce dyes in batik wastewater. ZnO was selected as the semiconductor in this study because it is more effective than TiO_2 in the treatment of batik wastewater [9]. The ZnO semiconductor is characterized by a wide direct band gap of 3.37 eV, an excitation binding energy of 60 meV, and can absorb either dark purple or borderline ultraviolet (UV) light at room temperature [10]. Additionally, ZnO is abundant, non-toxic, and has low production costs (75% lower than TiO_2) [11]. ZnO can be synthesized from several precursors such as zinc chloride [$ZnCl_2$] [12], zinc acetate dihydrate [$Zn(COOCH_3)_2 .2H_2O$] [13], and zinc sulfate heptahydrate [$ZnSO_4 .7H_2O$] [14]. However, these types of precursors often require other materials, either acids or bases, in their reaction [15], so it is considered less practical. To support the concept of green chemistry as an effort to reduce the use of chemicals excessively, we produce ZnO using Zn powder as a precursor because the transformation mechanism of Zn into ZnO is easy to carry out in a neutral solution such as distilled water, as seen in reactions (1) and (2) [16].

$$Zn_{(s)} + 2H_2O \rightarrow Zn(OH)_2 + 2H^+ + 2e^- \quad (1)$$

$$Zn(OH)_2 \rightarrow ZnO + H_2O \quad (2)$$

Reduced graphene oxide (rGO) is a graphene derivative with various applications, including sensors [17], supercapacitors [18], lithium-ion batteries [19], adsorbents [20], and photocatalysis [21]. Using rGO as a catalyst for wastewater decolorization offers a promising solution that addresses both efficiency and sustainability challenges. rGO exhibits high surface area and excellent electron transfer properties, enabling it to catalyze the degradation of dyes and other organic pollutants efficiently [21]. Combining rGO with ZnO can overcome the limitations of a single ZnO, resulting in improved efficiency [22]. In addition, rGO coupled with a semiconductor can accept photogenerated electrons to prevent the recombination, while also enhancing dye adsorption through $\pi - \pi$ conjugation between the dye molecules and the rGO surface [23]. Hence, this composite has the potential to reduce environmental pollution significantly. Furthermore, this study presents a novel approach to synthesizing an rGO/ZnO composite by utilizing GO and Zn powder without using additional chemical agents, offering a practical and scalable pathway for photocatalyst development.

In this study, we investigated the role of Zn powder as a precursor of ZnO and its impact on rGO in designing and evaluating efficient composites in photocatalytic activity. We also conducted a comparative analysis on two rGO/ZnO composites based on the variation of rGO, both containing 5% and 10%. We assessed the photocatalytic performance of the two composite materials in batik wastewater degradation under a UV lamp.

METHOD

Materials and Equipment

The materials employed in this research were Graphene oxide (ITNANO Laboratory, Indonesia), Zinc Powder (Merck, Germany), ZnO (Merck, Germany), distilled water, and Batik wastewater obtained from Kampung Batik Kamboje (Pontianak, Indonesia). The equipment used

in this research was a magnetic stirrer, an analytical balance, an ultrasonicator, a UV lamp (8-watt), an oven, and a photocatalyst reactor.

Synthesis of rGO/ZnO Composite

Firstly, GO at 5% (w/w) and 10% (w/w) was stirred with distilled water for two hours to break the sheets into small flakes. The resulting flakes were then ultrasonicated for four hours. After that, 20 grams of Zn powder were subsequently added to each variation of rGO suspension. The composite suspension was stirred for an additional two hours, then heated in an oven at 250°C for one hour until an rGO/ZnO composite was obtained.

Photocatalytic Activity Setup

A photocatalytic test was conducted to observe the performance of the rGO/ZnO composites in degrading dyes from batik wastewater using composite masses of 0.2, 0.4, and 0.8 grams. As much as 200 mL of batik wastewater was prepared, and the photocatalytic activity process was irradiated using a UV lamp while being continuously stirred with a magnetic stirrer for seven hours in a photocatalyst reactor. At one-hour intervals, 4 mL of waste samples were taken to measure the absorption spectrum and peak absorbance values using a UV-Vis spectrophotometer.

Performance Modeling of Photocatalytic Activity

The decolorization rate of batik wastewater during photocatalytic activity can be modeled using the pseudo-first-order kinetics [24], as seen in Equations (3) and (4). According to the Lambert-Beer Law, absorbance is directly proportional to concentration; therefore, concentration can be expressed in terms of absorbance for kinetic modeling. Here, A_0 and A_t represent the absorbance at t = 0 and t = time (hours), respectively. While, K_{App} is the degradation rate constant, and t is the time of photocatalysis.

$$\frac{A_t}{A_0} = e^{-K_{App}t} \tag{3}$$

$$\ln\frac{A_0}{A_t} = K_{App}t \tag{4}$$

The degradation efficiency (η) of the rGO/ZnO composite in treating dyes in batik wastewater was calculated using Equation (5), where A_0 is the initial absorbance before photocatalysis, and A_t is the absorbance during the photocatalysis process.

$$\eta\ (\%) = \frac{A_0 - A_t}{A_0} \times 100\% \tag{5}$$

RESULTS AND DISCUSSION

SEM-EDS Analysis

Figure 1(a) presents the surface morphology of commercial GO and Zn before the formation of composite. The GO displays a layered, sheet-like carbon structure with a relatively thick and stacked morphology, indicating a high content of oxygen functional groups as a result of oxidative treatment in synthesis of GO. In contrast, the Zn particles (Figure 1(b)) exhibit irregular morphologies in both shape and size. Figure 1 (c) and (d) show the surface morphology of the rGO/ZnO composites with variation of 5% and 10% rGO. The rGO appears as thin, sheet-like layers, while the ZnO particles are observed as spherical structures distributed across the rGO surface [25].

Based on SEM image observations, the increase in rGO content facilitates the formation of a greater amount of ZnO, as evidenced by the overlapping ZnO observed on the rGO surface at 10% concentration. The higher rGO content also provides a larger surface area, which facilitates the growth of ZnO particles. During the polymerization process, a higher rGO content promotes the formation of C–O–Zn bonds, which strengthen the interaction and enhance both the growth and distribution of ZnO on the rGO surface [26]. Additionally, the use of Zn powder as the starting material influences the crystallization behavior, thereby contributing to the morphological development on the resulting ZnO structures [27].

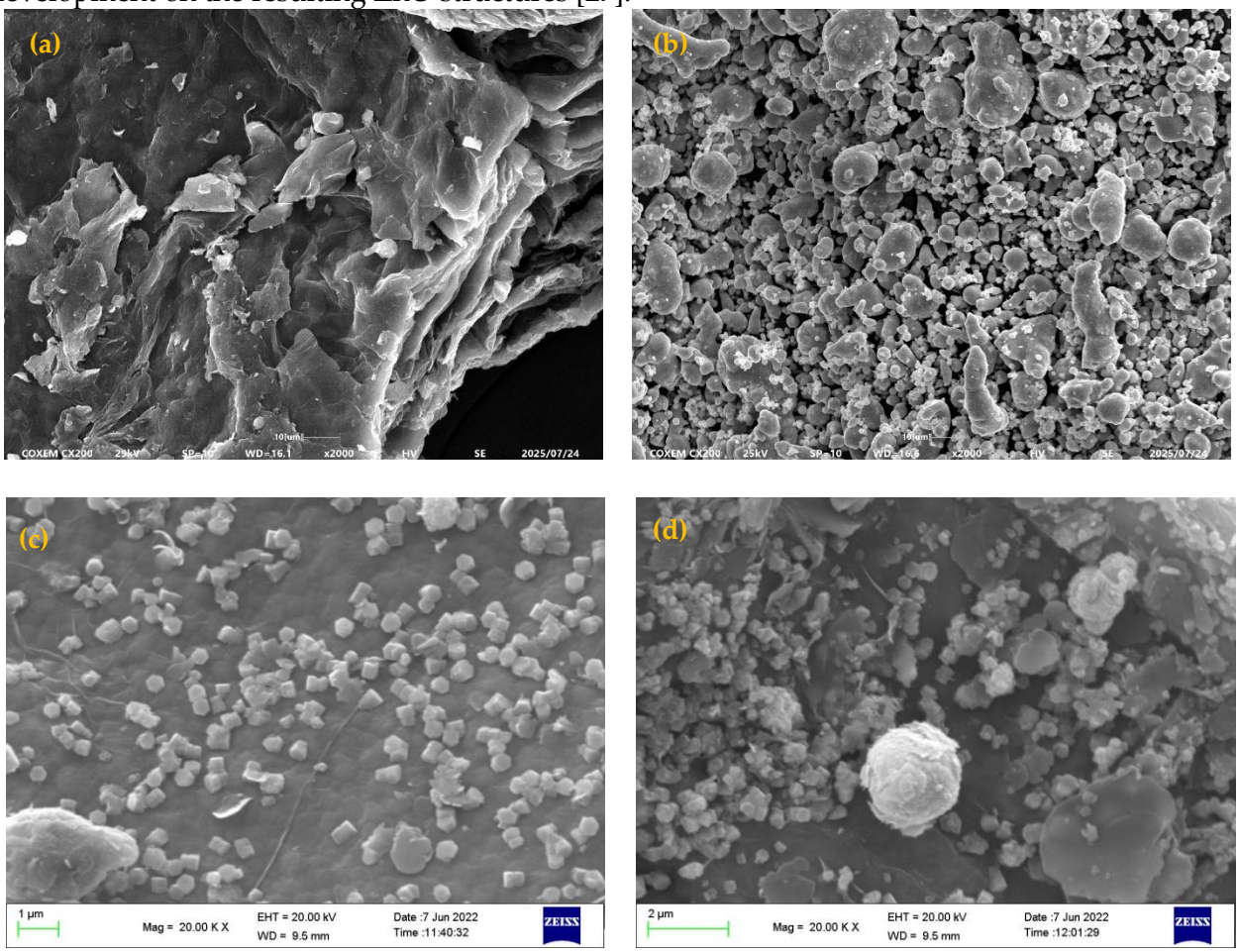

Figure 1. Surface morphology of: (a) GO, (b) Zn powder, (c) rGO/ZnO 5%, and (d) rGO/ZnO 10%

EDS characterization was conducted to determine the elemental composition of the materials. The EDS spectrum of GO (Figure 2(a)) revealed the presence of several impurity elements, including silicon with a mass percentage (wt.%) of 4.43%, aluminum 2.34%, sulfur 2.96%, potassium 1.49%, and iron 0.53%, in addition to the main components carbon at 47.90% and oxygen at 40.35%. These impurities, totaling approximately 12.88%, may originate from incomplete removal of sulfuric acid and potassium permanganate during the GO synthesis process, while additional contamination may arise from equipment-related sources. Meanwhile, the EDS spectrum of Zn (Figure 2(b)) exhibits well-defined and intense peaks, indicating its strong presence and dominance in the sample. The absence of impurities and the clarity of the spectral features suggest that the Zn employed in this study possesses a high degree of purity. Figure 2 (c) and 2 (d) present the EDS

analysis results, indicating Zn, C, and O as the main composition at the 5% and 10% rGO concentrations. At 5% rGO, the compositions (wt.%) were 43.99%, 39.77%, and 13.84%, respectively, while at 10% concentration they were 45.99%, 34.39%, and 16.13%. These data show a reduction in oxygen content in both samples compared to the initially high concentration of oxygen-containing functional groups in GO (40.35%). Increasing the rGO content to 10% (w/w) effectively doubles the amount of GO in the reaction system, without increasing the amount of reducing agent. As a result, the Zn powder becomes insufficient to reduce all oxygen-containing functional groups on the GO sheets, leading to a higher final oxygen content at 10% variation. This phenomenon reflects the dual role of Zn powder, which not only acts as a precursor for ZnO formation but also functions as a reducing agent for GO. As a precursor, Zn undergoes oxidation to form ZnO, that contribute to the photocatalytic and semiconducting properties of the composite. Simultaneously, Zn donates electrons that chemically reduce GO to rGO by removing oxygen-containing groups. The reduction process involves the elimination of oxygen-containing functional groups, accompanied by the evolution of gas bubbles that contribute to the exfoliation of GO layers [16].

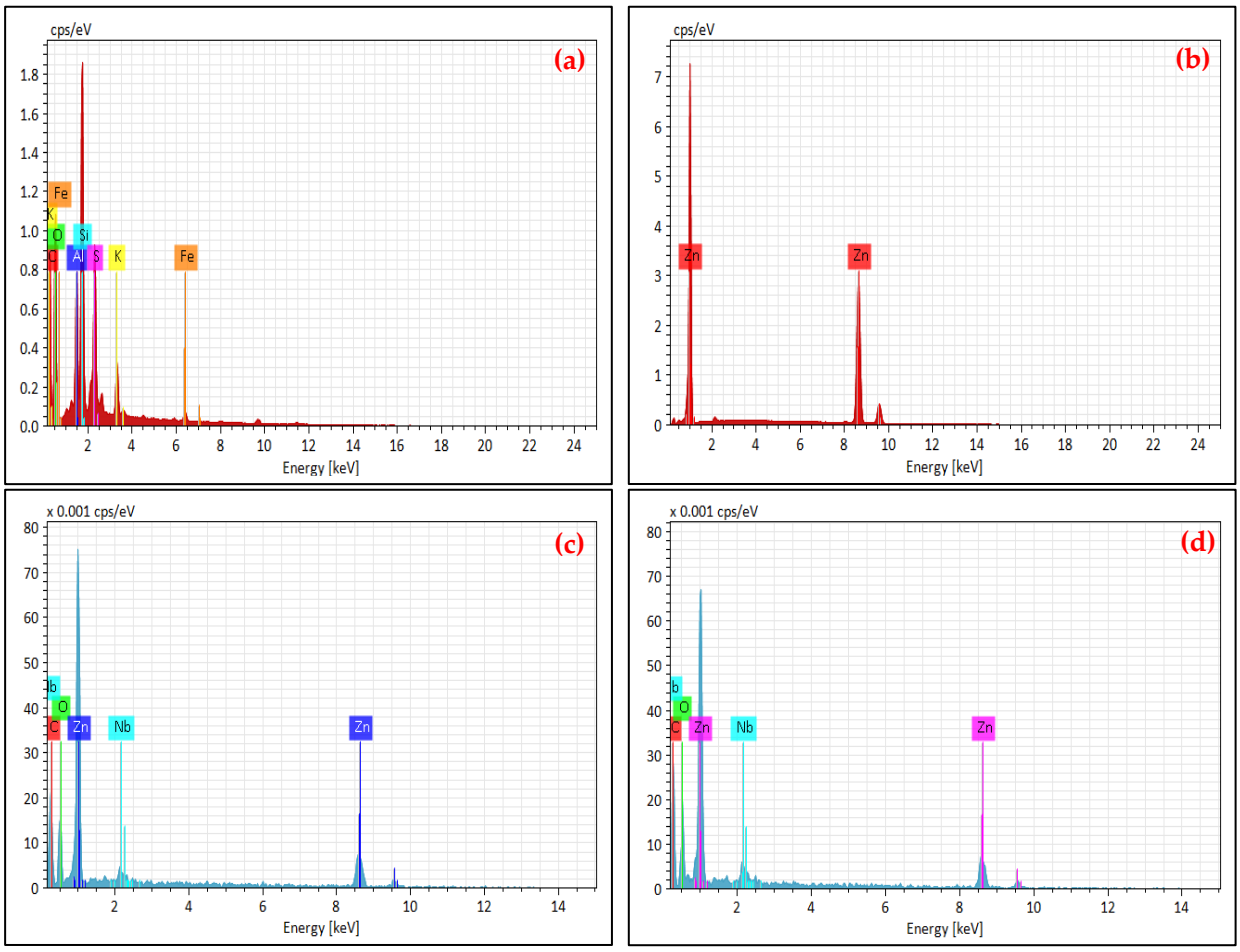

Figure 2. EDS spectrum of: (a) GO, (b) Zn powder, (c) rGO/ZnO 5%, and (d) rGO/ZnO 10%

The EDS in Figures 2 (c) and (d) also reveal the presence of impurity (niobium (Nb)) in small quantities. Nb was detected at 2.39% in the 5% rGO sample and increased to 3.49% in the 10% sample. While the exact source of Nb remains unclear, its increasing concentration at higher GO

content suggests a possible association with the GO precursor or contamination introduced during synthesis or handling. Notably, the increased impurity level in the 10% rGO/ZnO composite has a beneficial effect on its photocatalytic performance. These impurities can create defect states within the ZnO crystal lattice, which serve as trapping sites for photogenerated charge carriers. By facilitating charge separation and suppressing direct electron–hole recombination, these defect sites contribute to improved photocatalytic efficiency [28].

The carbon-to-oxygen (C/O) ratio is a key indicator of the successful conversion of GO to rGO. GO shows a C/O ratio of 1.58, which falls within the typical range for GO materials, between 1 and 2. After composite formation, the C/O ratios increase to 4.23 for rGO/ZnO 5% and 3.79 for rGO/ZnO 10%. These higher ratios are consistent with the commonly reported range for rGO (2.5–10), confirming that rGO was effectively formed in this study. The higher C/O ratio in the 5% composite suggests a more effective reduction process, likely due to the lower rGO content. With less rGO present, the Zn powder could interact more comprehensively, enabling a more uniform reduction of oxygen in the GO structure.

Table 1. The C/O ratio of GO and rGO/ZnO composite (5% and 10%)

Element	Atom (at. %)		
	GO	rGO-5%	rGO-10%
C	57.85	70.96	70.90
O	36.58	16.76	18.67
Ratio of C/O	1.58	4.23	3.79

XRD Analysis

The XRD pattern in Figure 3 displays the diffraction profiles of Zn, ZnO, and rGO/ZnO composites containing 5% and 10% rGO. The pure Zn sample (▲) exhibits sharp peaks at 2θ = 36.29°, 38.99°, and 43.22°, which correspond to the hexagonal crystal structure of metallic Zn (JCPDS No. 04-0831). Meanwhile, the ZnO peaks (*) appear at 2θ = 31.84°, 34.55°, 36.35°, 47.69°, and 56.74°, indicating the formation of the hexagonal wurtzite ZnO phase (JCPDS No. 36-1451).

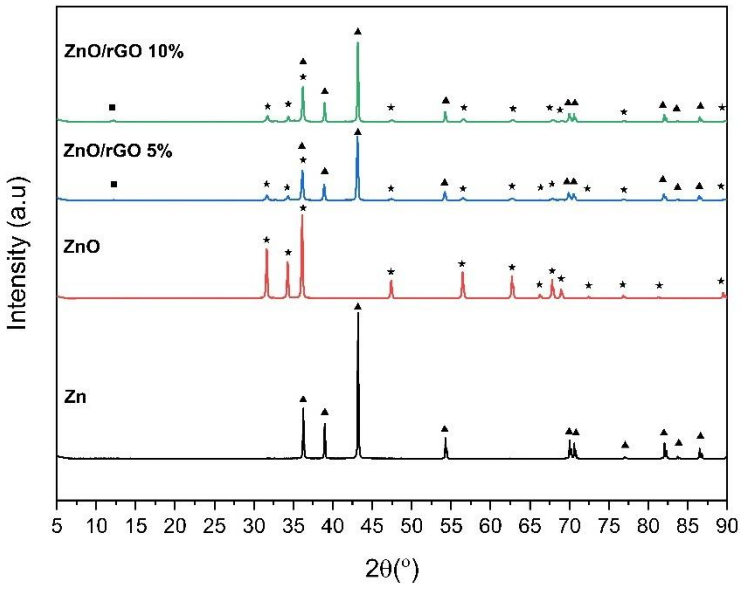

Figure 3. XRD Pattern of Zn, ZnO, and rGO/ZnO (5% and 10%)

In the rGO/ZnO composites, the ZnO peaks remain dominant. However, the presence of Zn peaks indicates that the oxidation process did not completely convert Zn to ZnO, consistent with previous studies that report complete oxidation typically occurs at 400℃ [29]. A weak peak is observed around $2\theta \approx 12°$ (marked with ■), indicating the presence of unreduced GO in both the 5% and 10% samples. Nonetheless, characteristic rGO peaks are not visible in the XRD patterns. This is likely due to the dominance of the sharp and intense diffraction peaks of Zn and ZnO, which overshadow the broad, semi-amorphous hump of rGO that typically appears at around $2\theta \approx 25°$ [30].

Effect of Adding rGO in the Composite

To investigate the effect of rGO on the rGO/ZnO composite, a comparative study was conducted using untreated and treated batik wastewater exposed to UV light for 7 hours. The photocatalytic performance was evaluated by adding 0.2 grams of either pure ZnO or rGO/ZnO composites (containing 5% and 10% rGO) into the batik wastewater samples. As shown in Figure 4, untreated batik wastewater exhibited no visible change after 7 hours of UV irradiation, confirming the necessity of a photocatalyst for dye degradation. When using pure ZnO, the dye absorbance decreased by only 4.55%, reflecting its limited photocatalytic efficiency. Similar results were previously reported, where single ZnO showed relatively low efficiency compared to rGO/ZnO composite with the variation of rGO [31]. In contrast, the rGO/ZnO composites demonstrated significantly enhanced performance. Incorporating 5% and 10% rGO into the ZnO structure resulted in a dye degradation efficiency of 38.79% and 42.02%, respectively. This notable improvement suggests that the incorporation of rGO enhances electron transfer, reduces charge recombination, and thereby increases the overall photocatalytic activity. Therefore, the rGO/ZnO composites, particularly at higher rGO content, outperformed single ZnO in degrading organic dyes in batik wastewater, underscoring the synergistic effect between rGO and ZnO in photocatalytic applications.

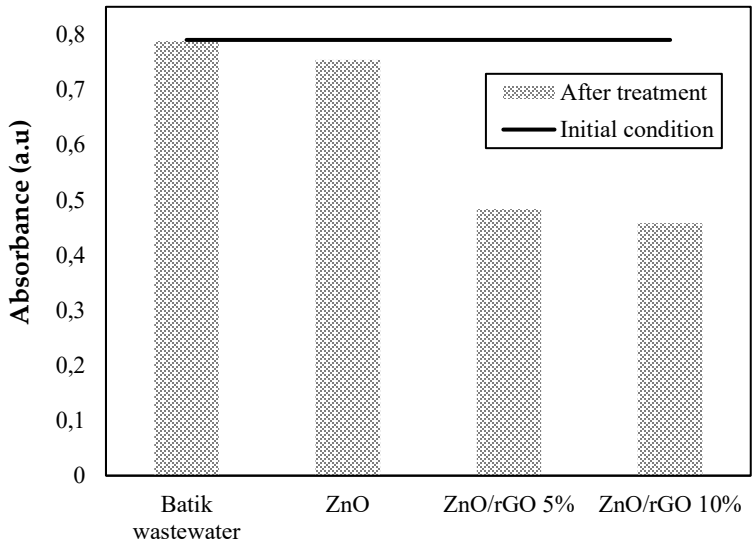

Figure 4. Comparison of photocatalytic activity between untreated and treated with ZnO, rGO/ZnO 5%, and rGO/ZnO 10%

As seen in Figure 5, the absorbance of batik wastewater increased within the first hour in both untreated and ZnO-treated batik wastewater samples. This is likely due to the formation of highly

reactive particles called free radicals, such as hydroxyl and superoxide radicals, which are generated when UV light interacts with the wastewater and ZnO. These radicals begin breaking down the large dye molecules in batik wastewater into smaller fragments. Some of these fragments absorb light more strongly than the original dyes, which explains the temporary increase in absorbance. For single ZnO, this effect is more noticeable because its photocatalytic activity is relatively low, meaning these light-absorbing fragments tend to build up before they can be fully broken down as a result of the rapid recombination of photogenerated electron–hole pairs of ZnO under UV irradiation [32]. This can be seen in the blue line in Figure 5, which shows the unstable performance of a single ZnO under UV lamp irradiation. Therefore, incorporating rGO into ZnO semiconductor is important because rGO helps suppress the charge recombination process of photogenerated electron-hole pairs in the photocatalytic activity [33].

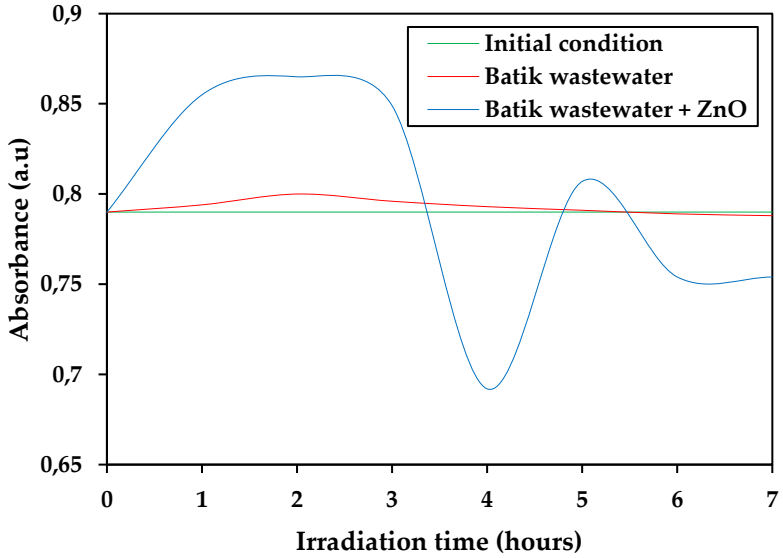

Figure 5. Phenomena of increasing the absorbance values of batik wastewater

Effect of Mass on Decolorization of Batik Wastewater

The mass of rGO/ZnO composite in batik wastewater is another important parameter in dye treatment, as it determines the total available active surface sites to optimize the interaction between the dye and the composite. Figure 6 shows the UV-Vis spectra (200-800nm) of batik wastewater after treatment. The control parameter (black line) showed a maximum wavelength of 508 nm, corresponding to remazol red dye [34]. The result shows that increasing the composite mass significantly reduces dye absorbance in batik wastewater. Adding rGO/ZnO composite mass to batik wastewater produces an effect similar to increasing the rGO in the composite. The 10% rGO variation generally exhibited better photocatalytic performance compared to the 5% variation due to its higher rGO content. However, when the mass of the 5% composite was increased to 0.8 grams, its photocatalytic activity surpassed that of the 10% composite at lower masses of 0.2 and 0.4 grams. This enhancement is due to the larger number of reactive surface sites, which facilitate the generation of active radicals and ultimately improve photocatalytic efficiency [8]. The optimal condition was observed for the 10% rGO composite at 0.8 grams (brown line), where a sharp decline in absorbance was seen after 7 hours of UV irradiation, indicating significant photocatalytic activity. To confirm the optimum mass from this experiment, an additional test was conducted by increasing the mass of a 10% composite as much as 1.2 grams to the batik wastewater. After 7 hours of UV

irradiation, the 0.8-gram sample achieved a higher efficiency of 67.91% compared to 1.2 grams, which was only 47.62%. Excessive catalyst loading can also reduce efficiency, because UV light cannot react optimally due to overlapping active sites.

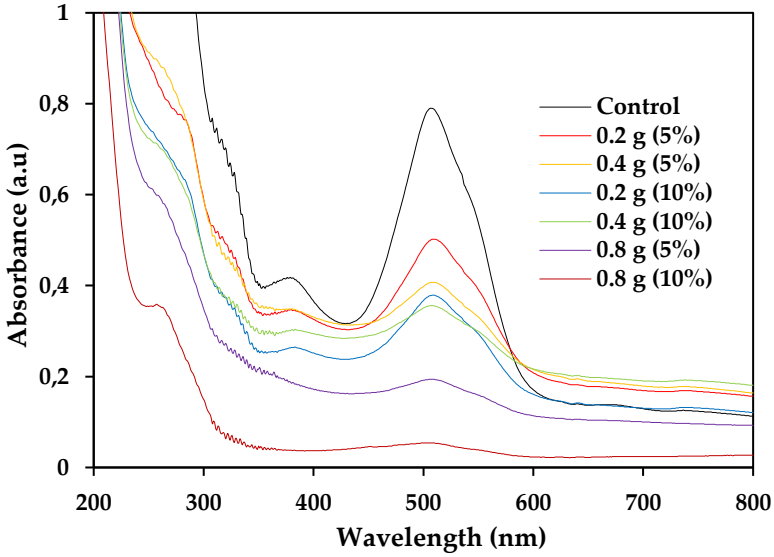

Figure 6. The UV-Vis spectrum of batik wastewater after 7 hours of treatment

Photocatalytic Activity: Pseudo-First-Order Kinetics and Composite Efficiency

To evaluate the reaction rate kinetics of the rGO/ZnO (5% and 10%) under different mass variations, the resulting experimental data were modeled using pseudo-first-order kinetics (Figures 7 and 8). The resulting data is not completely stable and shows slight fluctuations. This is most likely caused by rGO releasing absorbed dye back into batik wastewater, due to the desorption ability of rGO [35].

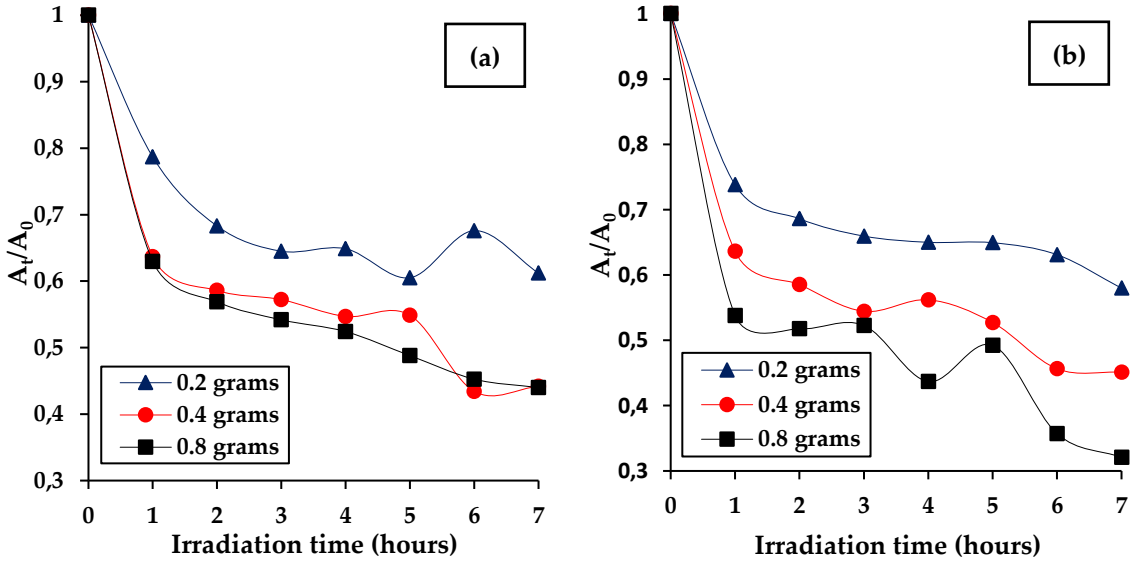

Figure 7. Plot of (A_t/A_0) as a function of time with varying mass; (a) 5% and (b) 10%

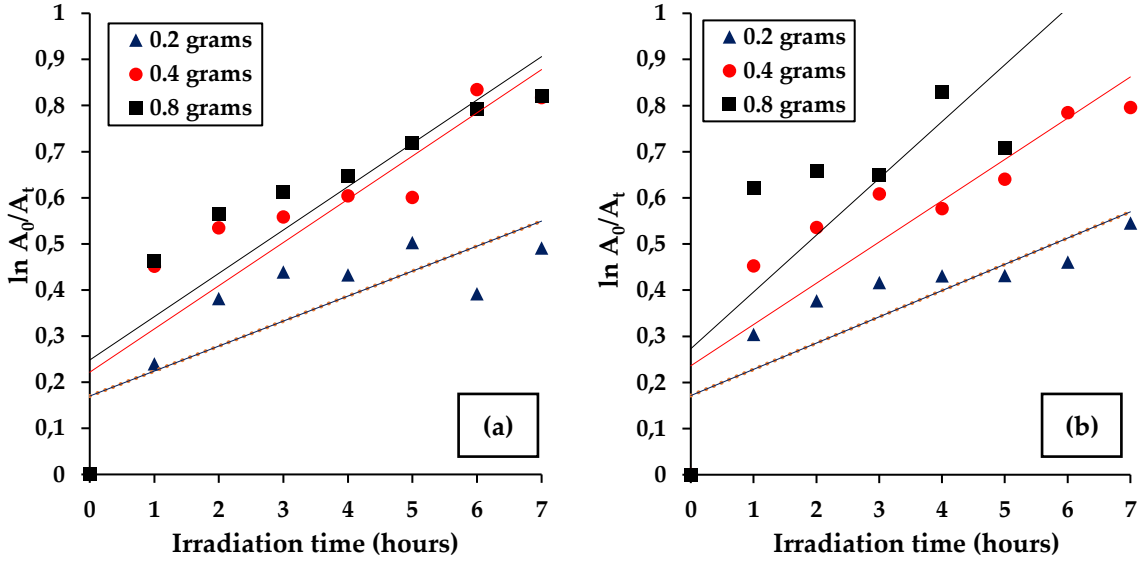

Figure 8. Plot of ln (A_0/A_t) as a function of time with varying mass; (a) 5% and (b) 10%

Apart from serving as a photocatalyst, rGO can also act as an adsorbent, which can adsorb other pollutants and dyes [36]. Previous studies have highlighted differences in the performance of rGO when functioning as an adsorbent compared to a photocatalyst. In adsorption tests, rGO can remove up to 91.74% of Indigo Carmine (IC) and 94.81% of Neutral Red (NR). Under photocatalytic conditions, the efficiency further increased to 98.74% for IC and 98.56% for NR. These increases, 7.63% for IC and 3.95% for NR, indicate that rGO exhibits not only adsorptive behavior but also photocatalytic activity [21]. However, once the rGO surface is filled with dyes, it becomes saturated and releases dyes back into the environment, increasing the absorbance value. When the surface is cleared, the dye begins to reoccupy the rGO pores, causing absorbance to decrease again. This phenomenon explains the slight fluctuation in the data.

The data fluctuation also caused the coefficient of determination (R^2) in Table 1 remain below one. The highest R^2 was obtained at a 5% concentration of 0.7855, indicating that this data is more stable than the others. The calculation of the reaction rate constant (K_{App}) obtained from $\ln(A_0/A_t)$ divided by time during photocatalysis is presented in Table 2 and plotted in Figure 8 (right). The highest rate constant corresponds to the optimal mass (0.8 grams) of 10% concentration.

Table 2. Determination coefficient ($\boldsymbol{R^2}$) and reaction rate constant ($\mathbf{K_{App}}$) after 7 hours of irradiation

Mass (grams)	rGO-5%		rGO-10%	
	$\boldsymbol{R^2}$	$\mathbf{K_{App}}$ (h^{-1})	$\boldsymbol{R^2}$	$\mathbf{K_{App}}$ (h^{-1})
0.2	0.6347	0.0701	0.7160	0.0778
0.4	0.7855	0.1167	0.7639	0.1136
0.8	0.7757	0.1173	0.7787	0.1623

The efficiency and reaction rate constant (K_{App}) shown in Figure 9 exhibit a linear relationship: the higher the efficiency, the higher the reaction rate constant. Figure 9 (left) shows the efficiency of 0.8-gram mass in both 5% and 10% concentrations, resulting in an efficiency of 56.01% and 67.91%, respectively. The reaction rate constant also peaked at the optimal mass (0.8 grams), reaching 0.1173 h^{-1} for 5% and 0.1623 h^{-1} for 10%. The relatively low dye removal efficiency observed

in this study contrasts with our previous findings, where an rGO/ZnO composite achieved reduction efficiencies of 99.83% for mercury and 91.82% for iron within 5 hours [37]. In another study, batik wastewater treated with TiO_2 coated on plastic granules achieved a degradation efficiency of up to 50.41% after 5 days of irradiation [7], indicating the inherent difficulty in degrading batik wastewater due to its complex composition. These results indicate that the rGO/ZnO composite performs effectively in degrading batik wastewater. Although not investigated in this research, the wax and resin residues from the batik washing process may influence the performance of the composite in decoloring, as such residues can adsorb onto the photocatalyst surface, forming a passivating layer that blocks light absorption and suppresses electron–hole pair generation [38].

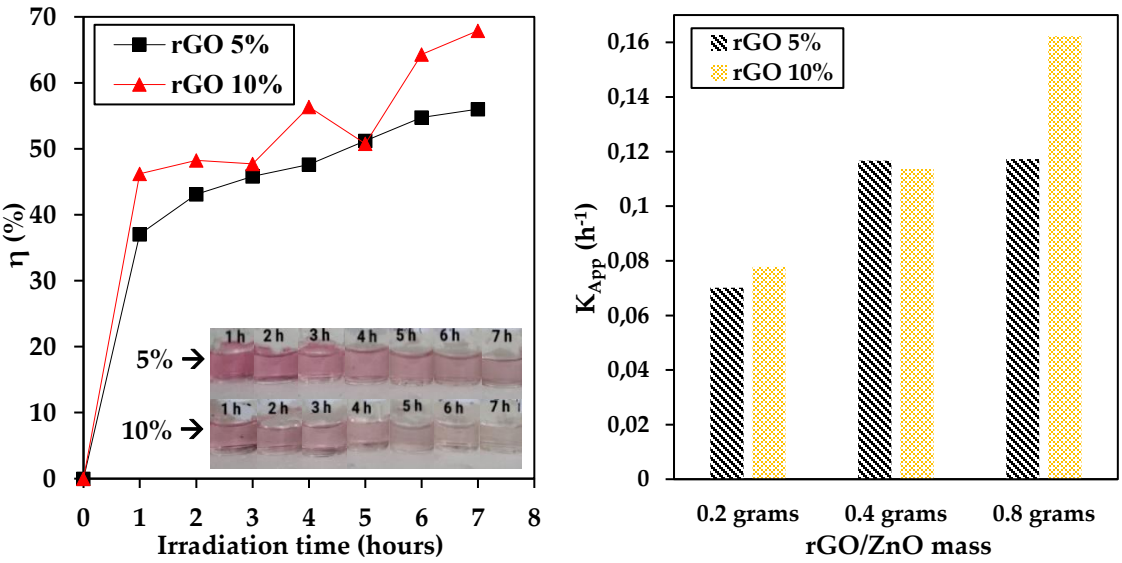

Figure 9. Efficiency (left) and reaction rate constant (right) after 7 hours of Irradiation

CONCLUSION

This study highlights the use of Zn powder as a precursor in synthesizing rGO/ZnO composites for batik wastewater treatment. SEM analysis revealed that rGO exhibits a sheet-like morphology, while ZnO appears as spherical particles with EDS characterization confirmed the presence of Zn, C, and O as the main elements, along with Nb detected as a minor impurity. Furthermore, the increase in the C/O ratio after rGO/ZnO formation also indicates the success of Zn as a reducing agent in transforming GO into rGO. XRD characterization verified the presence of ZnO in the composite, although residual Zn peaks were also observed, suggesting incomplete oxidation of the Zn precursor. Under UV irradiation, the rGO/ZnO composite exhibited better photocatalytic activity compared to pure ZnO. This enhancement is attributed to the ability of rGO in suppressing electron–hole recombination, thereby promoting more efficient photocatalytic reactions. Photocatalytic tests revealed that the composite containing 10% rGO with a mass of 0.8 grams represented the optimal condition for decolorization of batik wastewater. Thus, this study highlights several factors that influence photocatalytic performance, namely rGO concentration, composite mass, and irradiation time. Future studies could focus on optimizing the synthesis of rGO/ZnO to achieve complete oxidation of Zn precursors, exploring their visible-light activation to

expand application under solar irradiation, and investigating reusability and stability for long-term wastewater treatment, making the rGO/ZnO composite more practical for large-scale environmental remediation.

ACKNOWLEDGMENT

The authors would like to acknowledge DIPA FMIPA Universitas Tanjungpura for research funding in fiscal year 2024 through grant number SP DIPA-023.17.2.677517/2023 and contract number 1192/UN22.8/PT.01.05/2024. Mariani also thanks Comdev & Outreaching Universitas Tanjungpura and the Directorate General of Belmawa Kemenristekdikti.

AUTHOR CONTRIBUTIONS

Dwiria Wahyuni: Conceptualization, Methodology, Validation, Supervision, and Writing – Review and Editing; Mariani: Methodology, Investigation; Asifa Asri: Methodology, Supervision, and Writing - Original Draft, and Ya' Muhammad Arsyad: Investigation, Visualization, and Writing - Original Draft.

DECLARATION OF COMPETING INTEREST

The authors declare that they have no known competing financial interests or personal relationships that could have appeared to influence the work reported in this paper.

REFERENCES

[1] Yuliana, "Risiko Penggunaan Pewarna Sintetis pada Pewarnaan Batik untuk Kesehatan Pengrajin," Pros. Semin. Nas. Ind. Kerajinan dan Batik, pp. 1–6, 2022, [Online]. Available: https://proceeding.batik.go.id/index.php/SNBK/article/view/176

[2] S. Budiyanto, Anies, H. Purnaweni, and H. R. Sunoko, "Environmental Analysis of the Impacts of Batik Waste Water Polution on the Quality of Dug Well Water in the Batik Industrial Center of Jenggot Pekalongan City," E3S Web Conf., vol. 31, 2018, doi: https://10.1051/e3sconf/20183109008.

[3] B. Albiss and M. Abu-Dalo, "Photocatalytic Degradation of Methylene Blue using Zinc Oxide Nanorods Grown on Activated Carbon Fibers," Sustain., vol. 13, no. 9, pp. 1–15, 2021, doi: https://doi.org/10.3390/su13094729.

[4] K. Sirirerkratana, P. Kemacheevakul, and S. Chuangchote, "Color removal from wastewater by photocatalytic process using titanium dioxide-coated glass, ceramic tile, and stainless steel sheets," J. Clean. Prod., vol. 215, pp. 123–130, 2019, doi: https://10.1016/j.jclepro.2019.01.037.

[5] H. Bel Hadjltaief, M. Ben Zina, M. E. Galvez, and P. Da Costa, "Photocatalytic degradation of methyl green dye in aqueous solution over natural clay-supported ZnO-TiO2 catalysts," J. Photochem. Photobiol. A Chem., vol. 315, no. January, pp. 25–33, 2016, doi: https://10.1016/j.jphotochem.2015.09.008.

[6] S. Anita, T. A. Hanifah, G. F. Kartika, and P. H. Yanti, "Methylene Blue and Methyl Orange Dyes Removal using Low-Cost Composite of Banana Peel-TiO2Adsorbent," J. Phys. Conf. Ser., vol. 1819, no. 1, 2021, doi: https://10.1088/1742-6596/1819/1/012060.

[7] S. Sutisna et al., "Batik Wastewater Treatment Using TiO2 Nanoparticles Coated on the Surface of Plastic Sheet," Procedia Eng., vol. 170, pp. 78–83, 2017, doi: https://10.1016/j.proeng.2017.03.015.

[8] W. F. Khalik, L. N. Ho, S. A. Ong, Y. S. Wong, N. A. Yusoff, and F. Ridwan, "Decolorization and mineralization of Batik wastewater through solar photocatalytic process," Sains Malaysiana, vol. 44, no. 4, pp. 607–612, 2015, doi: https://10.17576/jsm-2015-4404-16.

[9] P. Chantes, C. Jarusutthirak, and S. Danwittayakul, "A Comparison Study of Photocatalytic Activity of TiO2 and ZnO on the Degradation of Real Batik Wastewater," 2015, doi: https://10.15242/iicbe.c0515033.

[10] C. B. Ong, L. Y. Ng, and A. W. Mohammad, "A review of ZnO nanoparticles as solar photocatalysts: Synthesis, mechanisms and applications," Renew. Sustain. Energy Rev., vol. 81, no. March 2017, pp. 536–551, 2018, doi: https://10.1016/j.rser.2017.08.020.

[11] A. S. Merlano, L. M. Hoyos, G. J. Gutiérrez, M. A. Valenzuela, and Á. Salazar, "Effect of Zn precursor concentration in the synthesis of rGO/ZnO composites and their photocatalytic activity," New J. Chem., vol. 44, no. 45, pp. 19858–19867, 2020, doi: https://10.1039/d0nj03683h.

[12] N. H. Mohammed and A. H. Al Khazraji, "Synthesis and study of zinc oxide nanoparticles and their nanocomposites," J. Pharm. Negat. Results, vol. 13, no. 4, pp. 790–797, 2022, doi: https://10.47750/pnr.2022.13.04.105.

[13] J. N. Hasnidawani, H. N. Azlina, H. Norita, N. N. Bonnia, S. Ratim, and E. S. Ali, "Synthesis of ZnO Nanostructures Using Sol-Gel Method," Procedia Chem., vol. 19, pp. 211–216, 2016, doi: https://10.1016/j.proche.2016.03.095.

[14] Sadraei R, "A Simple Method for Preparation of Nano-sized ZnO," Res. Rev. J. Chem. A, vol. 5, no. 2, pp. 45–49, 2016, doi: https://10.1016/S0008-6215(02)00353-1.

[15] S. Ningsih, M. Khair, and S. Veronita, "Synthesis and Characterization of ZnO Nanoparticles Using Sol-Gel Method," J. Chem. Sci, vol. 10, no. 1, pp. 59–68, 2021, [Online]. Available: http://journal.unnes.ac.id/sju/index.php/ijcs

[16] E. Kusrini, A. Suhrowati, A. Usman, M. Khalil, and V. Degirmenci, "Synthesis and Characterization of Graphite Oxide, Graphene Oxide, and Reduced Graphene Oxide from Graphite Waste using Modified Hummers Method and Zinc as Reducing Agent," Int. J. Technol., vol. 10, no. 6, pp. 1094–1102, 2019, doi: https://doi.org/10.14716/ijtech.v10i6.3639.

[17] K. Lee et al., "Highly selective reduced graphene oxide (rGO) sensor based on a peptide aptamer receptor for detecting explosives," Sci. Rep., vol. 9, no. 1, pp. 1–9, 2019, doi: https://10.1038/s41598-019-45936-z.

[18] Y. M. Volfkovich, A. Y. Rychagov, V. E. Sosenkin, S. A. Baskakov, E. N. Kabachkov, and Y. M. Shulga, "Supercapacitor Properties of rGO-TiO2 Nanocomposite in Two-component Acidic Electrolyte," Materials (Basel)., vol. 15, no. 21, pp. 1–17, 2022, doi: https://10.3390/ma15217856.

[19] C. Liu, T. Zhang, L. Cao, and K. Luo, "High-Capacity Anode Material for Lithium-Ion Batteries with a Core-Shell NiFe2O4/Reduced Graphene Oxide Heterostructure," ACS Omega, vol. 6, no. 39, pp. 25269–25276, 2021, doi: https://10.1021/acsomega.1c03050.

[20] K. Gupta and O. P. Khatri, "Reduced graphene oxide as an effective adsorbent for removal of malachite green dye: Plausible adsorption pathways," J. Colloid Interface Sci., vol. 501, no. April, pp. 11–21, 2017, doi: https://10.1016/j.jcis.2017.04.035.

[21] M. Shabil Sha et al., "Photocatalytic degradation of organic dyes using reduced graphene oxide (rGO)," Sci. Rep., vol. 14, no. 1, pp. 1–14, 2024, doi: https://10.1038/s41598-024-53626-8.

[22] D. Wahyuni, Nurhasanah, M. Nurhanisa, and Mariani, "Kinerja Fotokatalis Tunggal ZnO/Reduced Graphene Oxide (Zno/rGO) dibawah Iradiasi Sinar Matahari untuk Mendegradasi Metilen Biru," J. Ph J. Pendidik. Fis. dan Fis. Terap., vol. 4, no. 1, pp. 15–20, 2023,

doi: https://doi.org/10.22373/p-jpft.v9i1.17228.
[23] S. K. Mandal et al., "Engineering of ZnO/rGO nanocomposite photocatalyst towards rapid degradation of toxic dyes," Mater. Chem. Phys., vol. 223, no. June 2018, pp. 456–465, 2019, doi: https://10.1016/j.matchemphys.2018.11.002.
[24] I. Limón-rocha et al., "Effect of the Precursor on the Synthesis of ZnO and Its Photocatalytic Activity," Inorganics, vol. 10, no. 2, 2022, doi: https://10.3390/inorganics10020016.
[25] L. Zhu, Z. Liu, P. Xia, H. Li, and Y. Xie, "Synthesis of hierarchical ZnO&Graphene composites with enhanced photocatalytic activity," Ceram. Int., vol. 44, no. 1, pp. 849–856, 2018, doi: https://10.1016/j.ceramint.2017.10.009.
[26] K. H. V., N. C. S., T. R., G. D. Prasanna, N. G., and M. M. V., "An impact of RGO on the ZnO nanoparticles: structural, morphological, electrical, and gas sensing properties," Sens. Technol., vol. 2, no. 1, p., 2024, doi: https://10.1080/28361466.2024.2310479.
[27] N. Song, H. Fan, and H. Tian, "Reduced graphene oxide/ZnO nanohybrids: Metallic Zn powder induced one-step synthesis for enhanced photocurrent and photocatalytic response," Appl. Surf. Sci., vol. 353, pp. 580–587, 2015, doi: https://10.1016/j.apsusc.2015.06.062.
[28] A. M. Ilyas, J. D. Musah, S. W. Or, and A. O. Awodugba, "Precursor impurity-mediated effect in the photocatalytic activity of precipitated zinc oxide," J. Am. Ceram. Soc., vol. 107, no. 12, pp. 8269–8280, 2024, doi: https://10.1111/jace.20062.
[29] J. H. Lin et al., "Photoluminescence mechanisms of metallic Zn nanospheres, semiconducting ZnO nanoballoons, and metal-semiconductor Zn/ZnO nanospheres," Sci. Rep., vol. 4, pp. 1–8, 2014, doi: https://10.1038/srep06967.
[30] S. Abdolhosseinzadeh, H. Asgharzadeh, S. Sadighikia, and A. Khataee, "UV-assisted synthesis of reduced graphene oxide–ZnO nanorod composites immobilized on Zn foil with enhanced photocatalytic performance," Res. Chem. Intermed., vol. 42, no. 5, pp. 4479–4496, 2016, doi: https://10.1007/s11164-015-2291-z.
[31] W. M. Liu, J. Li, and H. Y. Zhang, "Reduced graphene oxide modified zinc oxide composites synergistic photocatalytic activity under visible light irradiation," Optik (Stuttg)., vol. 207, no. August, p. 163778, 2020, doi: https://10.1016/j.ijleo.2019.163778.
[32] Z. K. Bolaghi, S. M. Masoudpanah, and M. Hasheminiasari, "Photocatalytic activity of ZnO / RGO composite synthesized by one-pot solution combustion method," Mater. Res. Bull., vol. 115, no. January, pp. 191–195, 2019, doi: https://10.1016/j.materresbull.2019.03.024.
[33] B. Xue and Y. Zou, "High photocatalytic activity of ZnO–graphene composite," J. Colloid Interface Sci., vol. 529, no. April, pp. 306–313, 2018, doi: https://10.1016/j.jcis.2018.04.040.
[34] M. Hossein and H. Elahe, "Synthesis of cobalt-orthotitanate inverse spinel nano particles via a novel low temperature solvothermal method : structural , opto-electronical , morphological , surface characterization and photo-catalytical application in mineralization of Remazol Red ," J. Mater. Sci. Mater. Electron., vol. 0, no. 0, p. 0, 2017, doi: https://10.1007/s10854-017-6861-2.
[35] C. Z. Zhang, Y. Yuan, and T. Li, "Adsorption and Desorption of Heavy Metals from Water using Aminoethyl Reduced Graphene Oxide," Environ. Eng. Sci., vol. 35, no. 9, pp. 978–987, 2018, doi: https://10.1089/ees.2017.0541.
[36] J. Yang, S. Shojaei, and S. Shojaei, "Removal of drug and dye from aqueous solutions by graphene oxide: Adsorption studies and chemometrics methods," npj Clean Water, vol. 5, no. 1, pp. 1–10, 2022, doi: https://10.1038/s41545-022-00148-3.

[37] D. Wahyuni, Nurhasanah, Y. Muhammad Arsyad, and Mariani, "Removal of mercury and iron in water using reduced graphene oxide/zinc oxide composite," J. Phys. Conf. Ser., vol. 2945, no. 1, p. 012031, Jan. 2025, doi: https://10.1088/1742-6596/2945/1/012031.

[38] N. Zakaria, R. Rohani, W. H. M. Wan Mohtar, R. Purwadi, G. A. Sumampouw, and A. Indarto, "Batik Effluent Treatment and Decolorization—A Review," Water (Switzerland), vol. 15, no. 7, 2023, doi: https://10.3390/w15071339.